TOXICOLOGICAL SCIENCES **103(2)**, 335–345 (2008)
doi:10.1093/toxsci/kfn056
Advance Access publication March 15, 2008

In Vitro Assessment of Mitochondrial Dysfunction and Cytotoxicity of Nefazodone, Trazodone, and Buspirone

James A. Dykens,* Joseph D. Jamieson,† Lisa D. Marroquin,† Sashi Nadanaciva,‡ Jinghai J. Xu,§ Margaret C. Dunn,§ Arthur R. Smith,§ and Yvonne Will¶,[1]

**Drug Safety Research and Development, Pfizer, Inc., Sandwich, UK CT139NJ; †Drug Safety Research and Development, Pfizer, Inc., San Diego, California 92121; ‡MitoSciences, Inc., Eugene, Oregon 97403; §Systems Biology, Pfizer Research Technology Center, Pfizer, Inc., Cambridge, Massachusetts 02139; and ¶Exploratory Safety Differentiation, Pfizer, Inc., Eastern Point, Groton, Connecticut 06340*

Received January 24, 2008; accepted March 5, 2008

Mitochondrial toxicity is increasingly implicated in a host of drug-induced organ toxicities, including hepatotoxicity. Nefazodone was withdrawn from the U.S. market in 2004 due to hepatotoxicity. Accordingly, we evaluated nefazodone, another triazolopyridine trazodone, plus the azaspirodecanedione buspirone, for cytotoxicity and effects on mitochondrial function. In accord with its clinical disposition, nefazodone was the most toxic compound of the three, trazodone had relatively modest effects, whereas buspirone showed the least toxicity. Nefazodone profoundly inhibited mitochondrial respiration in isolated rat liver mitochondria and in intact HepG2 cells where this was accompanied by simultaneous acceleration of glycolysis. Using immunocaptured oxidative phosphorylation (OXPHOS) complexes, we identified Complex 1, and to a lesser amount Complex IV, as the targets of nefazodone toxicity. No inhibition was found for trazodone, and buspirone showed 3.4-fold less inhibition of OXPHOS Complex 1 than nefazodone. In human hepatocytes that express cytochrome P450, isoform 3A4, after 24 h exposure, nefazodone and trazodone collapsed mitochondrial membrane potential, and imposed oxidative stress, as detected via glutathione depletion, leading to cell death. Our results suggest that the mitochondrial impairment imposed by nefazodone is profound and likely contributes to its hepatotoxicity, especially in patients cotreated with other drugs with mitochondrial liabilities.

Key Words: **nefazodone; trazodone; buspirone; hepatotoxicity; mitochondria; drug toxicity.**

Nefazodone is a triazolopyridine antidepressant. Its efficacy is based on inhibiting the reuptake of serotonin by antagonizing the 5-hydroxytryptamine(serotonin) (5-HT) receptor 2 and also α1-adrenergic receptors (Eison *et al*., 1990; Taylor *et al*., 1995). Trazodone is also a triazolopyridine derivative that inhibits serotonin reuptake and also is a 5-HT2 receptor antagonist. The azaspirodecanedione anxiolytic and antidepressant buspirone is a 5-HT1A receptor partial agonist, and a mixed agonist/antagonist on postsynaptic dopamine receptors. Bristol-Myers Squibb discontinued the sale of nefazodone (“Serzone”) in the United States in 2004 due to hepatotoxicity with an incidence of 28.9/100,000 patients (Aranda-Michel *et al*., 1999; Choi, 2003; DeSanty and Amabile, 2007; Eloubeidi *et al*., 2000; Lucena *et al*., 2003). However, several generic formulations of nefazodone are still available.

In contrast, trazodone is associated with lower incidence of liver injury (DeSanty and Amabile, 2007), and adverse event reports on organ toxicity are rare for buspirone. Although the mechanisms of hepatotoxicity for trazodone have been attributed to a hypersensitivity mechanism (Beck *et al*., 1993; Chu *et al*., 1983; Fernandes *et al*., 2000; Hull *et al*., 1994; Longstreth and Hershman, 1985; Sheikh and Nies, 1983), the mechanism of idiosyncratic liver injury for nefazodone is not fully understood.

Nefazodone is metabolized by CYP3A4 (cytochrome P450, isoform 3A4), but also inhibits the enzyme which can lead to drug–drug interactions with numerous xenobiotics including statins and macrolides, many of which have their own mitochondrial liabilities (Alderman, 1999; Benazzi, 1997; Nadanaciva *et al*., 2007b). For example, most of the statins, except fluvastatin, are metabolized by CYP3A4 (Karnik and Maldonado, 2005). Trazodone only weakly inhibits CYP3A4 (Caccia, 2007).

Kostrubsky *et al*. (2006) reported inhibition of canicular transport with nefazodone, but not with trazodone or buspirone. C_{max} values of 2–4 μg/ml are reported in human plasma, and there are no data documenting the plasma-to-liver ratio of nefazodone, but if nefazodone accumulates in the liver it could potentially inhibit its own elimination (Kostrubsky *et al*., 2001). Indeed, reduced hepatic clearance has been reported in elderly women taking nefazodone (Caccia, 2007).

Recently it was reported that nefazodone preferentially inhibits Complex I of the electron transport system (Nadanaciva *et al*., 2007a). Here we expand upon this work by evaluating nefazodone, trazodone, and buspirone effects on isolated rat liver mitochondria, and on cytotoxicity to HepG2 cells grown

[1] To whom correspondence should be addressed. Fax: (860) 441-9637. E-mail: yvonne.will@pfizer.com.

with only galactose as respiratory substrate to render them more reliant on oxidative phosphorylation (OXPHOS) (Marroquin *et al*., 2007). Because HepG2 cells have little or no CYP3A4 activity, and because they are transformed cells derived from a tumor, the three drugs were also evaluated in primary human hepatocytes that express CYP3A4 (Wilkening *et al*., 2003) by monitoring mitochondrial membrane potential, cytotoxicity and cellular glutathione levels.

MATERIALS AND METHODS

Materials. All chemicals were purchased from Sigma-Aldrich (St Louis, MO) and Toronto Research Chemicals (Toronto, Canada) and were of the highest purity available. Phosphorescent oxygen-sensitive probe, type A65N-1, was from Luxcel Biosciences (Cork, Ireland). The BCA kit for protein determination was from Pierce (Rockford, IL). Black body clear bottom 96-well plates (Costar 3631) were purchased through VWR (Westchester, PA). Nunc Maxisorp clear bottom 96-well plates were purchased from Fisher. Protein G plates were from Pierce. All monoclonal antibodies were from MitoSciences Inc. (Eugene, OR). Cell culture media and supplements were purchased from Invitrogen (Carlsbad, CA), except for fetal bovine serum (FBS), which was purchased from Tissue Culture Biologics (Los Alamitos, CA). Culture flasks (BD Biocoat) and 96-well plates (BD Biocoat) were purchased from VWR. CellTiter-Glo Luminescent Cell Viability Assay kits were purchased from Promega (Madison, WI). Culture plates for metabolic profiling were obtained from Seahorse Biosciences (Chicopee, MA).

Animals. Care and maintenance were in accordance with the principles described in the Guide for Care and Use of Laboratory Animals (NIH Publication 85–23, 1985). Male Sprague–Dawley Rats (150–180 g) were purchased from Charles River (Wilmington, MA). Animals were housed in pairs in a controlled environment with constant temperature (21 ± 2°C) and a 12-h light/dark cycle. Food and water were available *ad libitum*. Animals were euthanized with an overdose of carbon dioxide. Organs were rapidly excised and placed into ice-cold mitochondrial isolation buffers (see below).

Cell Culture Conditions for HEPG2 Cells

High-glucose media. High-glucose Dulbecco's modified Eagle's medium (DMEM) (Invitrogen 11995-065) containing 25mM glucose and 1mM sodium pyruvate and supplemented with 5mM N-2-hydroxyethylpiperazine-N′-2-ethanesulfonic acid (HEPES), 10% FBS, and penicillin–streptomycin (pen–strep; 500 μg/ml final concentration).

Galactose media. DMEM deprived of glucose (Invitrogen 11966-025) supplemented with 10mM galactose, 2mM glutamine (plus 4mM in media prior to supplementation to yield total of 6mM), 5mM HEPES, 10% FBS, 1mM sodium pyruvate, and pen–strep as above.

HepG2 cells (ATTC, Manassas, VA) were grown in either glucose or galactose-containing media and kept in 5% CO_2 at 37°C. Cells were maintained on collagen-coated 150-cm^2 flasks (356486, BD Biocoat) and seeded onto 96-well plates for individual experiments.

Measurement of Cellular Adenosine Triphosphate Content in HepG2 Cells

Cells were plated at 40,000 cells/ml on collagen-coated, clear 96-well plates. The final media volume was 100 μl. Cellular adenosine triphosphate (ATP) concentrations were assessed by using the CellTiter-GloCell Viability Assay as per manufacturer's instructions. For drug treatments, compound stock solutions were prepared in dimethyl sulfoxide (DMSO) and added to the wells to give the indicated final drug concentrations. Final DMSO concentration was 0.5%. Drugs were added 24 h before measurements.

Metabolic Profiling

Growth medium. DMEM (Invitrogen 11995-065) containing 25mM glucose and 1mM sodium pyruvate and supplemented with 5mM HEPES, 10% FBS, and penicillin–streptomycin (pen–strep; 500 μg/ml final concentration).

Unbuffered medium. DMEM Base 8.3 g/l (Sigma-Aldrich D5030) supplemented with 2mM GlutaMax-1, 1mM sodium pyruvate, 25mM glucose, 31.58mM NaCl, and 15 mg of Phenol Red. Media was warmed to 37°C and the pH was adjusted to 7.4 using 5M KOH.

HepG2 cells were seeded in XF 24-well cell culture microplates at 7.5×10^4 cells/well in 250 μl of growth medium and then incubated at 37°C/5% CO_2 for 20–24 h. Assays were initiated by removing the growth medium from each well and replacing it with 750 μl of unbuffered medium prewarmed to 37°C. Cells were incubated at 37°C for 30 min to allow media temperature and pH to reach equilibrium before the first rate measurement. Prior to the rate measurements, the XF24 (Seahorse biosciences, North Billerica, MA) Analyzer gently mixed the assay media in each well for 10 min to allow the oxygen partial pressure to reach equilibrium. Following the mixing, the oxygen consumption rate (OCR) and extracellular acidification rate (ECAR) were measured simultaneously three times to establish a baseline rate. For each measurement there was a mix/wait time of about 5 min to restore normal oxygen tension and pH in the microenvironment surrounding the cells. After the baseline measurement, 75 μl of a testing agent prepared in assay medium was then injected into each well to reach the desired final concentration as indicated on the graphs. Multiple measurements as well as compound injections were made at the time points indicated. The values of OCR and ECAR reflect both the metabolic activities of the cells and the number of cells being measured. For relative measurements comparing metabolic rate after compound exposure to a pre-exposure baseline, that is, when data are expressed as a percentage of OCR or ECAR change over baseline, the number of cells present in a well does not confound analysis because the same cell population is assayed at each time interval, that is, paired comparison design.

Measurement of Respiration in Isolated Rat Liver Mitochondria

Liver mitochondria were isolated and oxygen consumption was monitored in 96-well plate format using a phosphorescent oxygen-sensitive probe as previously described (Hynes *et al*., 2006; Nadanaciva *et al*., 2007b; Will *et al*., 2006) with minor modifications. Briefly, A65N-1 oxygen probe was reconstituted in 10.5 ml of mitochondrial incubation buffer to a concentration of approximately 100nM. 100 μl of this solution were pipetted into each well of a 96-well plate (10 pmol of probe per well). For drug treatments, compound stock solutions were prepared in DMSO and added to the wells to give the indicated final concentrations (final DMSO < 0.5%). All drug concentrations are presented as nmol/mg of mitochondrial protein. After drug or vehicle addition, 50 μl of mitochondria stock solutions were added to each well giving the desired final concentration of mitochondria, followed by 50 μl of substrate (12.5/12.5mM glutamate/malate/malate final concentration) without or with adenosine diphosphate (ADP) (1.65mM final concentration) in incubation buffer. Finally, 100 μl of heavy mineral oil was added to each well to seal the samples from ambient oxygen, and the plate was placed in a fluorescence plate reader (Safire^2 Tecan, Innsbruck, Austria) equilibrated at 30°C and monitored over a period of 20 min measuring probe fluorescence signal in each well every 1.5 min in kinetic mode. Instrument settings were: 380/650 nm excitation/emission, filters, a delay time of 30 μs and a measurement window of 100 μs and active temperature control of the microplate compartment at 30°C. To ensure gas and temperature equilibration of samples at the start of the assay, all the dispensing steps were carried out at 30°C using prewarmed solutions and a Multi-Blok heater (Barnstead/LabLine, Melrose Park, IL) holding the microplate. After completion of fluorescence measurements, time profiles of fluorescence intensity in each well were analyzed using Magellan (Tecan, Insbruck, Austria) and Excel (Microsoft software, Redmond, WA to determine the rates of oxygen consumption based on the known relationship between probe fluorescence and oxygen concentration (Will *et al*., 2006). Rates of change of dissolved oxygen were subsequently determined from the slopes of these concentration profiles, over the initial 8 min.

Measurement of Activities of Individual OXPHOS Complexes

Bovine heart mitochondria were isolated according to Smith (1967). Activities of Complex I (nicotinamide adenine dinucleotide (reduced)-ubiquinone oxidoreductase), Complex II + III (succinate–cytochrome *c* oxidoreductase), Complex IV (cytochrome *c* oxidase), and Complex V (F_1Fo-ATPase) were all performed as previously described (Nadanaciva *et al*., 2007a, b).

For drug treatments, compound stock solutions were prepared in DMSO, added to multichannel Dilux Dilution Reservoirs (ISC BioExpress, Kaysville, UT) containing the appropriate assay solution and then dispensed into each 96-well plate in quadruplicate wells: in the Complexes I, IV, and V activity assays, measurements for a compound at a given concentration were done in triplicate wells coated with the appropriate immunocapture monoclonal antibody and a single well containing a null capture antibody (negative control); in the Complex II + III activity assay, measurements for a compound at a given concentration were done in triplicate wells with bovine heart mitochondria and a single well with no mitochondria (negative control). The final DMSO concentration in all these activity assays was 1.5% (vol/vol). This concentration of DMSO did not have an inhibitory effect in any of the assays. Each assay was read in a SpectraMax Plus^{384} plate reader immediately after addition of the assay solution (containing the drugs) to the 96-well plates. Absorbance values obtained during all activity assays on the SpectraMax Plus^{384} plate reader were exported from SoftmaxPro to either Excel or SigmaPlot. 100% activity (i.e. no inhibition) for each complex was determined as the mean of the triplicate measurement in absence of compound—negative control value in absence of compound. IC_{50} values were generated using a four-parameter logistic equation.

Human Hepatocyte Imaging Assay

Cryopreserved human hepatocytes were obtained commercially (CellzDirect; http://www.cellzdirect.com/). The cells were plated on collagen I–coated BD BioCoat 96-well plates in hepatocyte plating medium (Dulbecco's Minimal Essential Medium with 5% FBS; all media obtained from CellzDirect). Upon cell attachment, the medium was changed to hepatocyte culturing medium (Williams E medium, from CellzDirect). On the second day, the Matrigel overlay was applied according to CellzDirect recommended protocol. On the third day, the cells underwent a medium change with hepatocyte culturing medium. On the fourth day, the cells were treated overnight with the compound of interest or vehicle (0.1% DMSO). All compounds were initially solubilized in DMSO and diluted in culturing medium containing 5% FBS to a final DMSO concentration of 0.l%. After 24 h of incubation (37°C, 5% CO_2, 100% humidity), media were removed and the cells were stained by fluorescent probes in the same culturing medium lacking serum. The fluorescent probes were: tetramethyl rhodamine methyl ester for mitochondrial membrane potential (TMRM; 0.02μM, 1 h), 1,5-bis[[2-(dimethylamino)ethyl]amino]-4,8-dihydroxyanthracene-9,10-dione for nuclei and lipids DNA (DRAQ5; 45μM, 30 min), 5-(and-6)-chloromethyl-2′7′-dichlorodihydrofluorescein diacetate acetyl ester for reactive oxygen species (ROS) (CM-H_2DCFDA; 10μM, 30 min), and finally monochlorobimane for glutathione (mBCl; 80μM, 5 min). Automated live-cell multispectral image acquisition was performed on a Kinetic Scan Reader (Cellomics; http://www.cellomics.com/) using a 20x objective and an XF93 filter. The mBCl probe was added live on the deck of the instrument. The fluorescence images were captured according to the excitation and emission wavelengths of each probe:

- 655 ± 15 and 730 ± 25 nm for DRAQ5
- 475 ± 20 and 515 ± 10 nm for CM-H_2DCFDA
- 549 ± 4 and 600 ± 12.5 nm for TMRM
- 365 ± 25 and 515 ± 10 nm for mBCl

To capture enough cells (> 500) for analysis, six image fields starting from the center of a well were collected from each well. Image analysis was performed using ImagePro Plus software (Media Cybernetics, Bethesda, MD).

Statistics

For mitochondrial respiration measurements, the slopes of O_2 consumption during the initial 8 min of the reaction were analyzed via one-way ANOVA, followed by Tukey's *post hoc* test (GraphPad Prism 4). For ATP depletion and isolated mitochondrial respiration assays, IC_{50} values were generated using GraphPad Prism 4 or Sigma Plot.

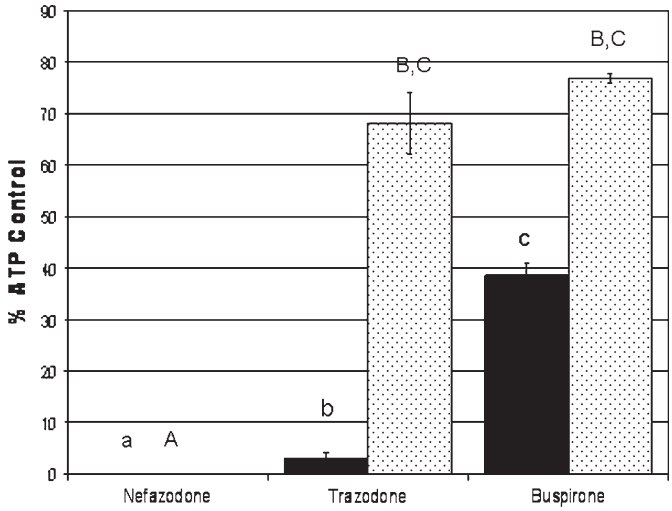

FIG. 1. Viability of HepG2 cells grown in either glucose (open bars) or galactose-containing media (black bars) exposed to 200μM nefazodone, trazodone, or buspirone for 24 h. ATP content was measured and expressed as percent of vehicle-treated controls. Data are mean ± SD ($n = 3$ separate experiments). Means not significantly different share superscripts (ANOVA $F = 900$, $p < 0.0001$, Bonferroni multiple comparison test; percentage data were transformed prior to ANOVA via $Y = (\ln)Y$).

RESULTS

Effect on ATP Content in Glucose and Galactose-Grown HepG2 Cells

Recently we have developed a cell model where HepG2 cells are cultured in media where glucose is replaced by galactose. Under these conditions the cells are more reliant on OXPHOS, thereby becoming susceptible to mitochondrial toxicants and to drugs with known mitochondrial liabilities (Marroquin *et al*., 2007). As such, these cells are better suited for assessments of drug-induced mitochondrial dysfunction. Here we evaluated Nefazodone, Buspirone and Trazodone in both cell lines to examine possible mitochondrial effects of the three compounds.

HepG2 cells grown in glucose and galactose-containing media were treated with 200μM of either nefazodone, trazodone or buspirone for 24 h (Fig. 1). At this concentration, nefazodone was the most toxic drug, depleting 100% of ATP in both, glucose and galactose-grown cells, trazodone showed severe toxicity in galactose-grown cells (> 90% depletion), but only showed moderate toxicity (< 50%) in glucose-grown cells. Buspirone was even less toxic; in galactose cells it exhibited moderate toxicity (60%) and it glucose-grown cells it exhibited no toxicity (Fig. 1). Due to nefazodone's detrimental effect at 200μM, we generated a full dose response curve

for this compound in both glucose- and galactose-grown cells (Fig. 2). As already shown for trazodone and buspirone, galactose-grown cells were much more susceptible to nefazodone treatment, but at much lower concentration than with the other two drugs. The IC_{50} values were 38.4 and 9μM for glucose- and galactose-grown cells, respectively (Fig. 2). The rank order of toxicity for the three compounds was therefore nefazodone > trazodone > buspirone.

Metabolic Profiling

The notion that the cytotoxicity exhibited by these molecules could be attributed to mitochondrial toxicity was further examined via simultaneously monitoring oxygen consumption and ECARs using Seahorse BioSciences technology as described in materials and methods (Fig. 3). Rotenone, a potent respiratory Complex I inhibitor, was included as a positive control, and a DMSO vehicle treatment as a negative control. At 6.25μM (first injection), nefazodone profoundly inhibited oxygen consumption (OCR, Fig. 3A), accompanied by a compensatory increase in ECAR (Fig. 3B). These responses were worsened by the second injection, yielding 12.5μM concentration, but less of a response was noted with subsequent injections of drug. Similar, but less severe, responses were observed with trazodone and buspirone (25μM after each injection; 100μM after final injection). In accord with the viability data of galactose-grown cells (Fig. 1), trazodone is slightly more toxic than buspirone.

Effect on Oxygen Consumption by Isolated Rat Liver Mitochondria

The higher toxicity of all compounds in galactose-grown cells, plus decreased oxygen consumption and increased acidification, strongly suggest mitochondrial inhibition as a possible mechanism of toxicity. To further test this hypothesis, the three compounds were evaluated by monitoring respiration of isolated rat liver mitochondria. Mitochondrial oxygen consumption measurements were performed in two different states: State 2, where oxidizable substrates (glutamate/malate or succinate) are provided in the absence of exogenous ADP, and State 3, where both substrates and ADP are provided. At 200 nmol/mg protein, nefazodone profoundly and significantly inhibited glutamate/malate-driven basal State 2, and even more potently State 3, respiration (Fig. 4). In contrast, at the same concentration, trazodone showed a significant, but relatively modest, inhibition of State 2 respiration. Buspirone was indistinguishable from controls. The rank order of mitochondrial impairment for the three compounds is: nefazodone >> trazodone > buspirone. Basal State 2 respiration fueled by succinate, a substrate that provides electrons to Complex II thereby bypassing Complex I, was also inhibited by nefazodone, but only at the two highest concentrations (data not shown). Such inhibition independent of Complex I suggests a second, less potent, mechanism of inhibition. Neither trazodone nor buspirone had any effect on succinate-fueled respiration.

In light of the effect of nefazodone, dose response curves were generated for nefazodone starting at 100 nmol/mg protein (Fig. 5). Figure 5A shows the dose dependent effect on basal respiration, whereas Figure 5B corroborates the more potent effect on ADP-driven State 3 respiration noted above. The IC_{50} values were 16.7 nmol/mg protein and 9.8 nmol/mg protein for glutamate/malate basal and ADP-driven respiration, respectively, and the IC_{50} for basal succinate respiration is > 100 nmol/mg mitochondrial protein.

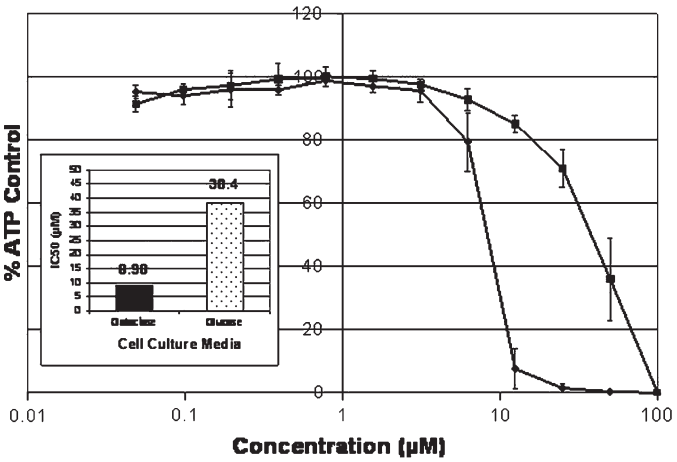

FIG. 2. HepG2 cells grown in either glucose (closed square) or galactose (closed diamond)media were incubated with the indicated concentrations of nefazodone. As reflected by the left shift in the curve, galactose-grown cells were significantly more susceptible to nefazodone treatment (IC_{50} = 8.98μM) compared with cells grown in glucose media (IC_{50} = 38.40μM). Data are mean ± SD (n = 3).

Target Identification

The potency of nefazodone to impair respiration fueled by glutamate/malate versus succinate suggests that Complex I could be a likely target, or perhaps adenine nucleotide translocase. Accordingly, we evaluated the effects of the drugs on the individual OXPHOS complexes. This was initially determined at 150μM, and a 9-point dose response, using twofold dilutions, was performed if an effect was observed.

When tested for inhibition of Complexes I, II/III, IV, and V activity, nefazodone potently inhibited Complex I, with an IC_{50} of 14μM (Table 1, Fig. 6). Buspirone showed 3.4-fold less inhibition resulting in an IC_{50} of 48μM for Complex I. Trazodone had no effect on Complex I activity. No Complex II/III inhibition was observed for any of the three antidepressants (Table 1). Complex IV was inhibited by nefazodone (IC_{50} 70μM), but not by trazodone or buspirone (Fig. 7), rendering this a likely candidate for the respiratory inhibition with succinate observed in isolated mitochondria. No complex V inhibition was observed for any of the three compounds (Table 1). The rank order of potency for the three drugs is: nefazodone > buspirone > trazodone.

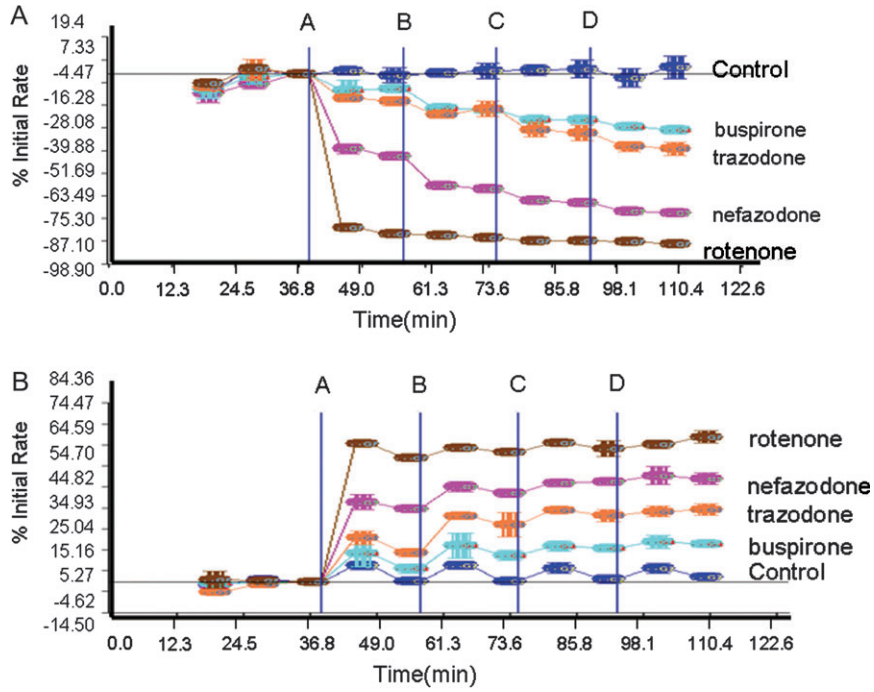

FIG. 3. Metabolic profiling reveals a decrease in oxygen consumption (OCR) upon exposure to nefazodone, trazodone, buspirone (A; rotenone is a positive control, and DMSO is vehicle control). This is accompanied by an increase in acidification rate (ECAR) as glycolysis accelerates to compensate for reduced respiration (B). Data are collected simultaneously, and nefazodone, trazodone, buspirone and rotenone were injected to 6.25, 25, 25, and 1.25μM final concentrations, respectively, at each of the time points A, B, C, and D. For example, after four injections, cells are exposed to 25μM nefazodone.

Effects on Primary Cultures of Human Hepatocytes

The potential cytotoxic effects of the three antidepressants were tested in sandwich-cultured primary human hepatocytes for 24 h at 100× their single-dose therapeutic C_{max} values (average systemic serum C_{max} after a single oral dosing; Table 2, bottom row). This yields concentrations of 92μM for nefazodone, 505μM for trazodone, and 0.5μM for buspirone. Figure 8 shows representative images of the same field of hepatocytes stained by DRAQ5 for nuclei and intracellular lipids (first column), CM-H_2DCFDA for ROS (second column), TMRM for mitochondrial membrane potential (third column), and mBCl for intracellular glutathione (fourth column). Under this treatment condition, primary human hepatocytes treated with 0.1% DMSO vehicle (Fig. 8, top row) exhibited normal round-shaped nuclear morphology, a basal level of ROS (a basal level of oxidized DCF signal sequestered into the bile canaliculi compartment with very little intracellular fluorescence), healthy mitochondria with normal mitochondrial membrane potential (perinuclear mitochondrial accumulation and intensity of TMRM signals), and normal intracellular reduced glutathione (mBCl fluorescence throughout the cytoplasm). Primary human hepatocytes treated with buspirone produced similar imaging results as the DMSO vehicle (Fig. 8, bottom row). On the other hand, hepatocytes treated with nefazodone resulted in significant cell loss (Fig. 8, first column, second row), increased ROS in some remaining cells (Fig. 8, second column, second row), near complete abolishment of the mitochondrial membrane potential even in the remaining cells (Fig. 8, third column, second row), and dramatic depletion of intracellular reduced glutathione (Fig. 8, last column, second row). Interestingly, trazodone also induced significant cell loss, mitochondrial damage, and loss of glutathione, although induction of ROS was not observed (Fig. 8, third row).

DISCUSSION

Of the three antidepressants evaluated, the data indicate that nefazodone is cytotoxic to HepG2 cells grown in either glucose or galactose, although the latter are significantly more susceptible. This was also the case for trazodone, and to a lesser extent buspirone which had only modest toxicity to glucose-grown cells. This potency rank order was corroborated via metabolic profiling and via monitoring respiration of isolated rat liver mitochondria. When respiration was fueled by succinate, inhibition by nefazodone was apparent at only the two highest concentrations, suggesting that Complex I is a primary site of inhibition, but that there is probably another mechanism of inhibition. This was confirmed using immunocaptured OXPHOS complexes, where nefazodone potently inhibited not only Complex I, but also, albeit less potently, Complex IV. In primary human hepatocytes that express

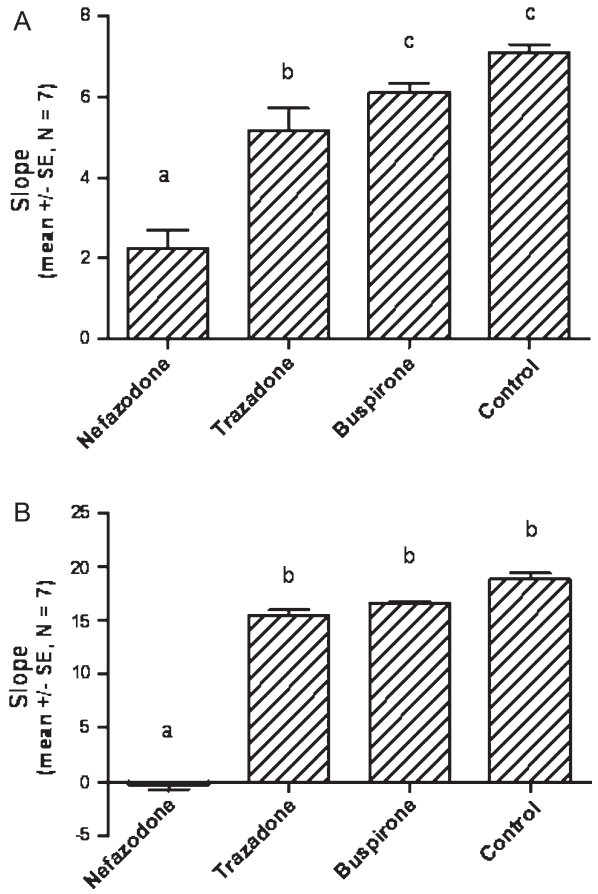

FIG. 4. Oxygen consumption by isolated rat liver mitochondria was severely inhibited by nefazodone. (A) The effect of nefazodone, trazodone, and buspirone (all at 200 nmol/mg mitochondrial protein) on basal glutamate/malate-driven State 2 respiration. (B) Effects on ADP-stimulated State 3 respiration. Letters indicate statistically significant differences between treatment groups as analyzed by ANOVA. Data are mean ± SE ($n = 7$).

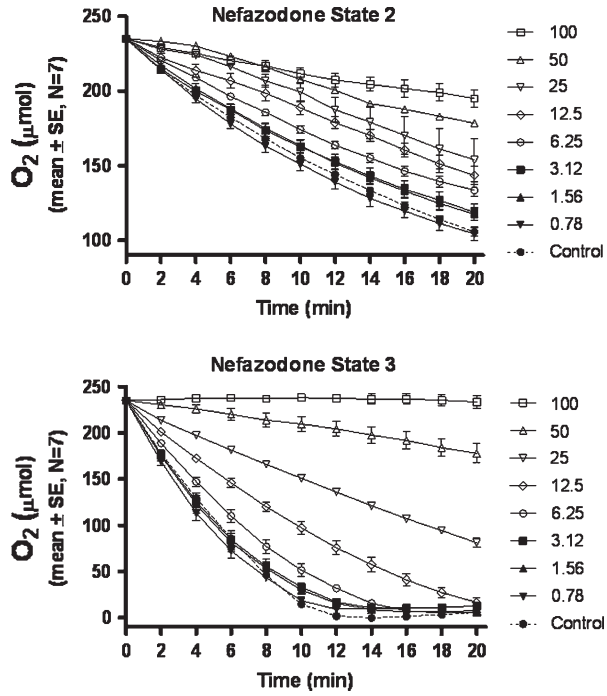

FIG. 5. Nefazodone inhibits basal and ADP-stimulated respiration in isolated liver mitochondria in a dose depend matter. (A) Effects on basal glutamate/malate-driven basal State 2 respiration at the drug concentrations indicated. (B) Effects on ADP-stimulated State 3 respiration. Data are mean ± SE ($n = 7$ separate experiments).

CYP3A4, 24-h exposure to nefazodone and trazodone collapses mitochondrial membrane potential, depletes glutathione and kills the cells.

In toto, the rank order of cyto- and mito-toxicity is nefazodone > trazodone > buspirone. This is in accord with the clinical disposition of these drugs, with nefazodone associated with more frequent and serious instances of hepatotoxicity (reviewed by DeSanty and Amabile, 2007). However, this inference, although justified, must also be informed by bioavailability of the three drugs, which varies widely: at the same oral dose, C_{max} values of 2–4 μg/ml are reported in human plasma, and there are no data documenting the plasma-to-liver ratio of nefazodone, but if nefazodone accumulates in the liver it could potentially inhibit its own elimination (Kostrubsky *et al.*, of nefazodone is in a similar range as trazodone, and more than 100-fold higher than buspirone (Table 2). Thus, tissue exposure to nefazodone can approach 10μM, rendering the cytotoxicity and other deleterious effects observed here more pathologically germane than those observed with buspirone that were primarily detected at nonpharmacological concentrations. This is particularly the case given the acute exposures used in some of our studies (see below). In this context, the effects of buspirone on immunocaptured respiratory Complex I may not be relevant to cytotoxicity given its lower dose and exposures *in vivo* (Table 2). It is interesting to note that at both 100-fold the orally administered single-dose human therapeutic C_{max} values of 2–4 μg/ml are reported in human plasma, and there are no data documenting the plasma-to-liver ratio of nefazodone, but if nefazodone accumulates in the liver it could potentially inhibit its own elimination (Kostrubsky *et al.*, values, both nefazodone and trazodone caused collapse of mitochondrial membrane potential, intracellular glutathione depletion, and significant cytotoxicity.

TABLE 1
IC_{50} Values for Inhibition of Immunocaptured Respiratory Complexes I, II/III, IV, and V.

Complex	Nefazodone	Trazodone	Buspirone
I	14μM	No effect	48μM
II/III	No effect	No effect	No effect
IV	70μM	No effect	No effect
V	No effect	No effect	No effect

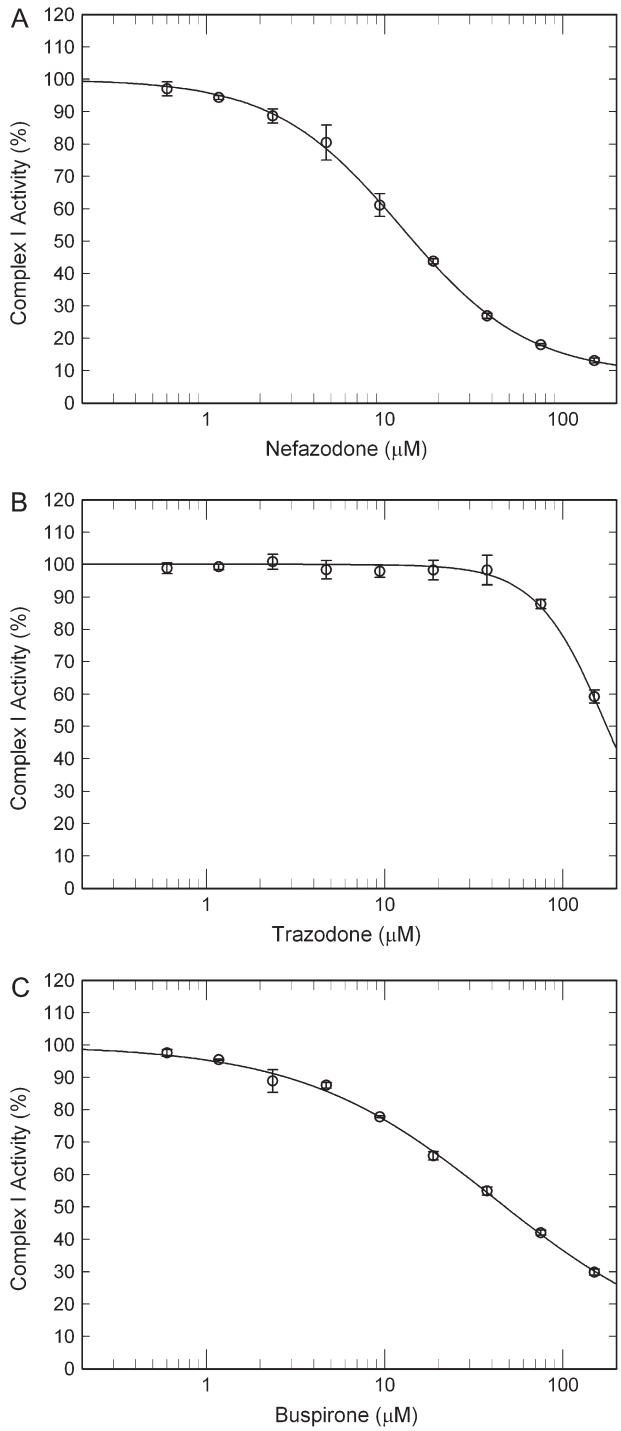

FIG. 6. IC_{50} curves for nefazodone (A), trazodone (B), and buspirone (C) on OXPHOS Complex I. Data are mean ± SD ($n = 3$ separate experiments).

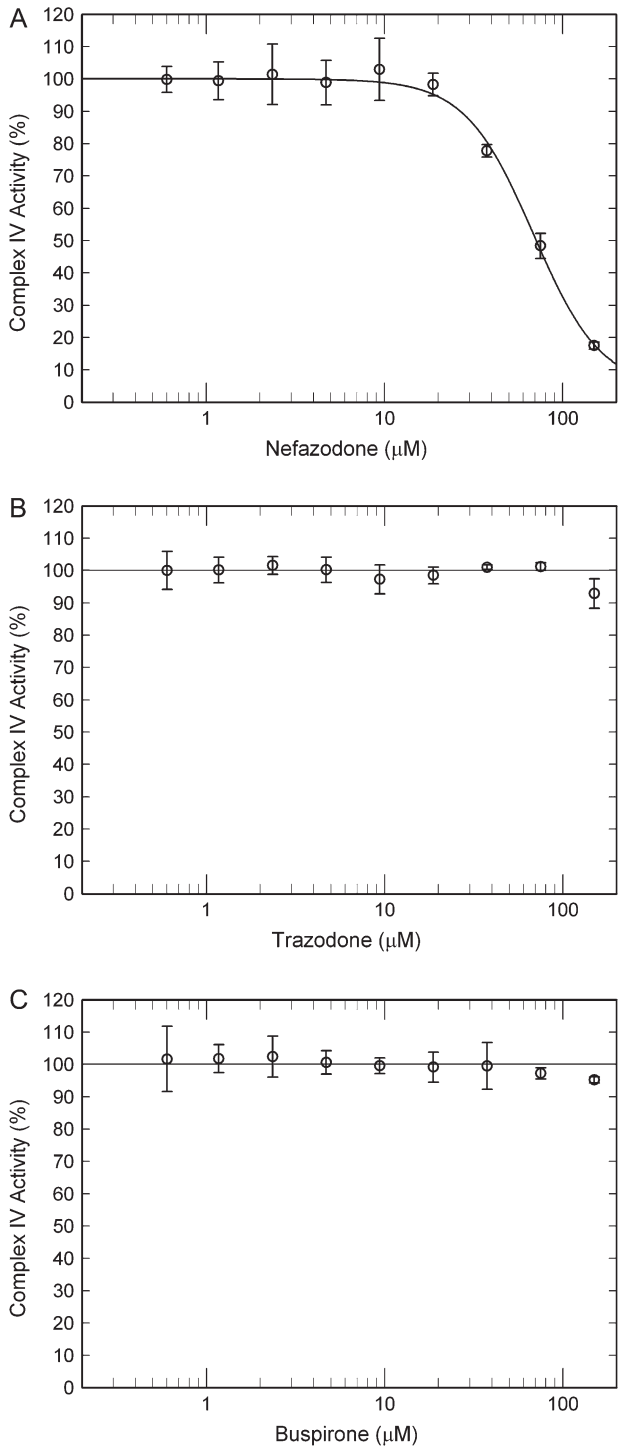

FIG. 7. IC_{50} curves for nefazodone (A), trazodone (B), and buspirone (C) on OXPHOS complex IV. Data are mean ± SD ($n = 3$ separate experiments).

It should be noted that drug exposures in both the HepG2 and human hepatocyte studies were conducted in the presence of serum, so that potential tight protein binding appears not to limit availability. Similarly, the parent molecules (nefazodone and/or trazodone) inhibited isolated mitochondria and isolated respiratory complexes, and were cytotoxic to HepG2 cells lacking CYP3A4, and to human hepatocytes that express it Wilkening *et al.*, 2003). As such, metabolism by CYP3A4 is apparently not required for toxicity. Interestingly, trazodone was generally less toxic than nefazodone in all the models used

TABLE 2
Dosing Regimen and C_{max} Values for Nefazodone, Trazodone, and Buspirone

Parameter	Nefazodone	Trazodone	Buspirone
Daily dose	100–200 mg in two divided doses	50–200 mg in two divided doses	10–30 mg in two divided doses
Dose/C_{max}	50 mg b.i.d./270 ng/ml 100 mg b.i.d./730 ng/ml 200 mg b.i.d./2050 ng/ml	50 mg/840 ng/ml 100 mg/1880 ng/ml	10 mg/0.9 ng/ml 20 mg/1.7 ng/ml 40 mg/3.0 ng/ml
Single-dose serum C_{max} for IVIVC	434 ng/ml, 0.92μM (Barbhaiya *et al*., 1995)	1880 ng/ml, 5.05μM (Nilsen and Dale, 1992)	1.92 ng/ml, 0.005μM (Skar and Andheria, 2001)

Note. For IVIVC, we used serum C_{max} from healthy volunteers after a single dose of 100 mg nefazodone and trazodone, but 20 mg for buspirone (bottom row). Notice that for nefazodone, higher C_{max} values have been reported after b.i.d. versus single dose. In our attempts to better predict idiosyncratic liver injury in humans, we exposed primary cultures of human hepatocytes to 100 times these C_{max} values. Total C_{max} values were used in this case, because of the presence of significant amounts of both serum proteins and Matrigel in the hepatocyte culture. Thus, 100 times of these C_{max} values approximate maximal hepatic exposures after oral administration in a diverse population. IVIVC, *in vitro in vivo* correlation.

here except the human hepatocytes where it was equally as toxic as nefazodone. Although admittedly a surrogate, this model more closely approximates clinical reality in that drug metabolism can occur. It bears reiteration that idiosyncratic liver injuries have been reported for trazodone (DeSanty and Amabile, 2007), and the data from the human hepatocytes suggest that drug metabolism may contribute to such toxicity. However, because the drugs were evaluated in the human hepatocyte model at 100-fold over C_{max} values of 2–4 μg/ml are reported in human plasma, and there are no data documenting the plasma-to-liver ratio of nefazodone, but if nefazodone accumulates in the liver it could potentially inhibit its own elimination (Kostrubsky *et al*., trazodone was tested at a dose at least five times higher than in the other assays, which could account for its toxicity being more apparent in this model.

The requirement for an elevated exposure in the *in vitro* setting to identify deleterious hepatic effects of these drugs may be due to a combination of: (1) liver exposure to an orally dosed drug can be an order of magnitude higher than its systemic exposure; (2) population pharmacokinetic variability due to age, genetics (including metabolism), and drug–drug interactions could further exacerbate local liver exposure and toxicity; (3) idiosyncratic organ history (including disease and previous drug exposures); (4) onset of hepatotoxicity in vivo is typically much longer than in vitro (see below), fostering dose escalation in most in vitro systems. Indeed, even the systemic C_{max} values of 2–4 μg/ml are reported in human plasma, and there are no data documenting the plasma-to-liver ratio of nefazodone, but if nefazodone accumulates in the liver it could potentially inhibit its own elimination (Kostrubsky *et al*., values can vary widely for nefazodone based on dose administered (Table 2) and patients' age groups (Barbhaiya *et al*., 1995).

There is growing evidence that drugs associated with organ toxicities have disproportionate extents of mitochondrial liabilities (Chan *et al*., 2005; Wallace and Starkov, 2000). For many antivirals and antibiotics, such toxicity is attributable to long-term inhibition of mitochondrial replication and gene expression (Wallace and Starkov, 2000). However, drugs with known organ toxicities are increasingly being found to directly inhibit and/or uncouple mitochondrial respiration (Chan *et al*., 2005; Dykens and Will, 2007; Dykens *et al*., 2007; Hynes *et al*., 2006; Nadanaciva *et al*., 2007b; Szewczyk and Wojtczak, 2002; Wallace and Starkov, 2000). For example, the thiazolidinediones variously inhibit and/or uncouple mitochondrial respiration in accord with their toxicity profiles (Nadanaciva *et al*., 2007b). Similarly, the rhabdomyolysis that limits the use of statins also parallels their acute and direct inhibition of mitochondrial respiration (Nadanaciva *et al*., 2007b).

The model that is emerging is one where "off target" impairment of mitochondrial function precipitates cytotoxicity once a bioenergetic threshold is crossed (Boelsterli, 2003; Dykens and Will, 2007; Dykens *et al*., 2007; Nadanaciva *et al*., 2007b; Wallace and Starkov, 2000). Most cells have robust energetic reserves, and can accelerate ATP production in response to a host of normal or noxious stimuli. That ability to respond to stressors is gradually eroded by drugs that impair mitochondrial function until a point where the cell can no longer generate the ATP needed for survival, and it dies. It should be noted in this context that many drugs induce elevations of serum alanine aminotransferase, a direct reflection of hepatocellular death, and many of these drugs have mitochondrial liabilities (Boelsterli, 2003; Dykens and Will, 2007).

In this model of drug toxicity via mitochondrial dysfunction, the deleterious effects on mitochondria are likely a fixed value, occurring in most patients to the same extent. The factors that contribute to idiosyncratic susceptibility are organ history and capacity to compensate for loss of mitochondrial capacity,

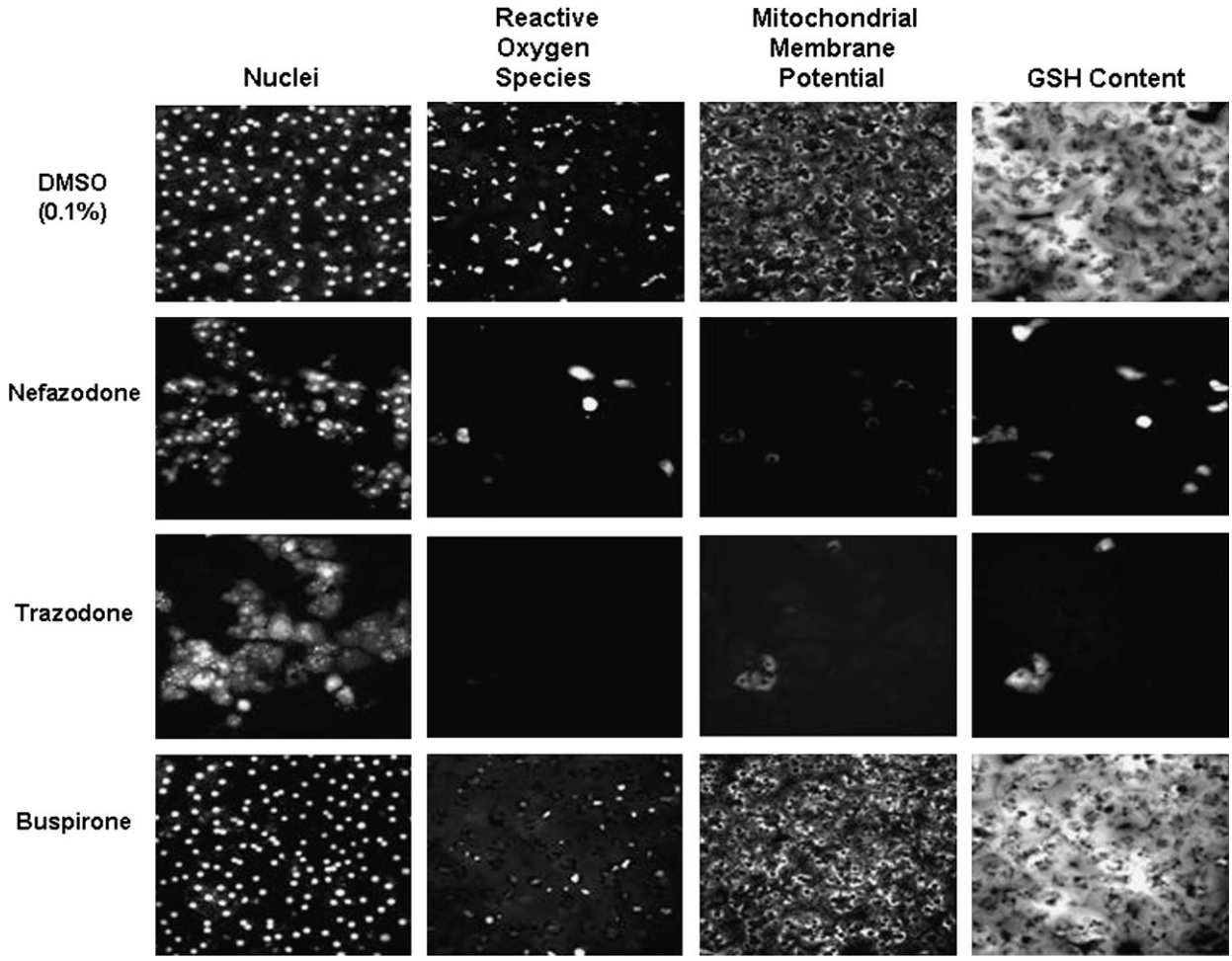

FIG. 8. Representative images of hepatocytes treated 24 h with 0.1% DMSO (top row), nefazodone (second row), trazodone (third row), buspirone (bottom row), all at 100× C_{max} (see Table 2), and stained with DRAQ5 for nuclei and intracellular lipids (first column), CM-H_2DCFDA for ROS (second column), TMRM for mitochondrial membrane potential (third column), and mBCl for intracellular glutathione (fourth column). The images from each row are obtained from the same image field of the same treatment sample.

which in turn has a genetic basis dictated by both the nuclear and mitochondrial genomes. Estimates of mitochondrial half-lives vary, but mitochondrial replacement occurs on a time scale of days-to-weeks. Given this time scale, even mild drug-induced mitochondrial impairment can gradually accumulate, amplifying the deleterious consequences of acute drug exposure. It bears reiteration that the time scales and drug concentrations used in our models reflect experimental expediency much more than the realities of pathophysiology. For example, cytotoxicity was assessed only after 24 h exposures, and it is feasible that longer exposures at lower doses could have exacerbated toxicity. Moreover, many drugs can be bioaccumulated by transmembrane carriers at the plasma membrane and at the mitochondrial membranes. For example, the statins paradoxically induce apoptosis in anaerobically poised, fast-twitch fibers, and not in mitochondrially enriched slow-twitch fibers, because of a selective membrane transporter on the susceptible fibers that takes up the statin (Dykens *et al*., 2007; Westwood *et al*., 2005). Indeed, cations can also bioaccumulate into the mitochondrial matrix because of the strong (approx. 220 mV) mitochondrial membrane potential, further exacerbating deleterious consequences (Dykens and Will, 2007; Dykens *et al*., 2007).

In addition to the bioenergetic threshold, drug-induced mitochondrial impairment can yield toxicity via other routes. For example, respiratory impairment increases the time the various OXPHOS remain in the reduced state, correspondingly increasing the probability of untoward autooxidation and univalent O_2 reduction to yield superoxide and other ROS or reactive nitrogen species (Brown and Borutaite, 2007). Similarly, under some conditions, uncoupling can also increase mitochondrial ROS formation (Dykens, 1994). In our models,

depending on the time scales, such increased free radical formation is detected directly, but also secondarily via glutathione depletion which serves as a longer-term index of cellular redox status. The known idiosyncratic hepatotoxin troglitazone very potently impairs mitochondrial respiration (Dykens *et al*., 2007; Nadanaciva *et al*., 2007b), but hepatotoxicity is not apparent in preclinical animal models. Only when the mitochondrial form of superoxide dismutase is knocked down by 50% is the hepatoxicity of troglitazone revealed *in vivo* (Ong *et al*., 2007). In this light, organ toxicity with a mitochondrial etiology is also a consequence of the equilibrium between radical formation and antioxidant capacity. In this case, however, the threshold is the antioxidant status of the cell.

Of course, the bioenergetic and antioxidant thresholds are metabolically and genetically connected, but they illustrate that drug-induced mitochondrial impairment can injure and kill cells in a myriad of ways. And they also underscore the importance of mitochondrial assessments in preclinical drug development programs, and the need for more models that better predict potential organ toxicity earlier in the drug development process.

REFERENCES

Alderman, C. P. (1999). Possible interaction between nefazodone and pravastatin. *Ann. Pharmacother* **33,** 871.

Aranda-Michel, J., Koehler, A., Bejerano, P. A., Poulos, J. E., Luxon, B. A., Khan, C. M., Ee, L. C., Balistreri, W. F., and Weber, F. L. (1999). Nefazodone-induced liver failure: Report of three cases. *Ann. Intern. Med.* **130,** 285–288.

Barbhaiya, R. H., Marathe, P. H., Greene, D. S., Mayol, R. F., Shukla, U. A., Gammans, R. R., Pittman, K. A., and Robinson, D. (1995). Safety, tolerance and preliminary pharmacokinetics of nefazodone after administration of single and multiple oral doses to healthy adult male volunteers: A double-blind phase I study. *J. Clin. Pharmacol.* **35,** 974–984.

Beck, P. L., Bridges, R. J., Demetrick, D. J., Kelly, J. K., and Lee, S. S. (1993). Chronic active hepatitis associated with trazodone therapy. *Ann. Intern. Med.* **118,** 791–792.

Benazzi, F. (1997). Dangerous interaction with nefazodone added to fluoxetine, desipramine, venlafaxine, valproate and clonazepam combination therapy. *J. Psychopharmacol.* **11,** 190.

Boelsterli, U. A. (2003). Diclofenac-induced liver injury: A paradigm of idiosyncratic drug toxicity. *Toxicol. Appl. Pharmacol* **192,** 307–322.

Brown, G. C., and Borutaite, V. (2007). Nitric oxide and mitochondrial respiration in the heart. *Cardiovasc. Res.* **75,** 283–290.

Caccia, S. (2007). N-dealkylation of arylpiperazine derivatives: Disposition and metabolism of the 1-aryl-piperazines formed. *Curr. Drug Metab* **8,** 612–622.

Chan, K., Truong, D., Shangari, N., and O'Brien, P. J. (2005). Drug-induced mitochondrial toxicity. *Expert Opin. Drug Metab. Toxicol.* **1,** 655–666.

Choi, S. (2003). Nefazodone (Serzone) withdrawn because of hepatotoxicity. *CMAJ.* **169,** 1187.

Chu, A. G., Gunsolly, B. L., Summers, R. W., Alexander, B., McChesney, C., and Tanna, V. L. (1983). Trazodone and liver toxicity. *Ann. Intern. Med.* **99,** 128–129.

DeSanty, K. P., and Amabile, C. M. (2007). Antidepressant-induced liver injury. *Ann. Pharmacother.* **41**(7), 1201–1211.

Dykens, J. A. (1994). Isolated cerebellar and cerebral mitochondria produce free radicals when exposed to elevated Ca^{2+} and Na^{+}: Implications for neurodegeneration. *J. Neurochem.* **63,** 584–591.

Dykens, J. A., Marroquin, L. D., and Will, Y. (2007). Strategies to reduce late-stage drug attrition due to mitochondrial toxicity. *Expert Rev. Mol. Diagn.* **7,** 161–175.

Dykens, J. A., and Will, Y. (2007). The significance of mitochondrial toxicity testing in drug development. *Drug Discov. Today* **12,** 777–785.

Eison, A. S., Eison, M. S., Torrente, J. R., Wright, R. N., and Yocca, F. D. (1990). Nefazodone: Preclinical pharmacology of a new antidepressant. *Psychopharmacol. Bull.* **26,** 311–315.

Eloubeidi, M. A., Gaede, J. T., and Swaim, M. W. (2000). Reversible nefazodone-induced liver failure. *Dig. Dis. Sci.* **45,** 1036–1038.

Fernandes, N. F., Martin, R. R., and Schnenker, S. (2000). Trazodone-induced hepatotoxicity: A case report with comments on drug-induced hepatotoxicity. *Am. J. Gastroenterol.* **95,** 532–535.

Hull, M., Jones, R., and Bendall, M. (1994). Fatal hepatic necrosis associated with trazodone and neuroleptic drugs. *BMJ* **309,** 378.

Hynes, J., Marroquin, L. D., Ogurtsov, V. I., Christiansen, K. N., Stevens, G. J., Papkovsky, D. B., and Will, Y. (2006). Investigation of drug-induced mitochondrial toxicity using fluorescence-based oxygen-sensitive probes. *Toxicol. Sci.* **92,** 186–200.

Karnik, N. S., and Maldonado, J. R. (2005). Antidepressant and statin interactions: A review and case report of simvastatin and nefazodone-induced rhabdomyolysis and transaminitis. *Psychosomatics* **46,** 565–568.

Kostrubsky, S. E., Strom, S. C., Kalgutkar, A. S., Kulkarni, S., Atherton, J., Mireles, R., Feng, B., Kubik, R., Hanson, J., Urda, E., *et al*. (2006). Inhibition of hepatobiliary transport as a predictive method for clinical hepatotoxicity of nefazodone. *Toxicol. Sci.* **90,** 451–459.

Kostrubsky, V. E., Vore, M., Kindt, E., Burliegh, J., Rogers, K., Peter, G., Altrogge, D., and Sinz, M. W. (2001). The effect of troglitazone biliary excretion on metabolite distribution and cholestasis in transporter-deficient rats. *Drug Metab. Dispos.* **29,** 1561–1566.

Longstreth, G. F., and Hershman, J. (1985). Trazodone-induced hepatotoxicity and leukonychia. *J. Am. Acad. Dermatol.* **13,** 149–150.

Lucena, M. I., Carvajal, A., Andrade, R. J., and Velasco, A. (2003). Antidepressant-induced hepatoxicity. *Expert Opin.* **2,** 249–262.

Marroquin, L. D., Hynes, J., Dykens, J. A., Jamieson, J. D., and Will, Y. (2007). Circumventing the crabtree effect: Replacing media glucose with galactose increases susceptibility of HepG2 cells to mitochondrial toxicants. *Toxicol. Sci.* **97,** 539–547.

Nadanaciva, S., Bernal, A., Aggeler, R., Capaldi, R., and Will, Y. (2007a). Target identification of drug induced mitochondrial toxicity using immunocapture based OXPHOS activity assays. *Toxicol. In Vitro* **21,** 902–911.

Nadanaciva, S., Dykens, J. A., Bernal, A., Capaldi, R. A., and Will, Y. (2007b). Mitochondrial impairment by PPAR agonists and statins identified via immunocaptured OXPHOS complex activities and respiration. *Toxicol. Appl. Pharmacol.* **38,** 33–42.

Nilsen, O. G., and Dale, O. (1992). Single dose pharmacokinetics of trazodone in healthy subjects. *Pharmacol. Toxicol.* **71,** 150–153.

Ong, M. M., Latchoumycandane, C., and Boelsterli, U. A. (2007). Troglitazone-induced hepatic necrosis in an animal model of silent genetic mitochondrial abnormalities. *Toxicol. Sci.* **97,** 205–213.

Sheikh, K. H., and Nies, A. S. (1983). Trazodone and intrahepatic cholestasis. *Ann. Intern. Med.* **99,** 572.

Skar, A., and Andheria, M. (2001). A comparative multidose pharmacokinetic study of buspirone extended-release tablets with a reference immediate-release product. *J. Clin. Pharmacol.* **41,** 886–894.

Smith, A. L. (1967). Preparation, properties, and conditions for assay of mitochondria: Slaughterhouse material, small-scale. *Methods Enzymol*. **10,** 81–86.

Szewczyk, A., and Wojtczak, L. (2002). Mitochondria as a pharmacological target. *Pharmacol. Rev*. **54,** 101–127.

Taylor, D. P., Carter, R. B., Eison, A. S., Mullins, U. L., Smith, H. L., Torrente, J. R., Wright, R. N., and Yocca, F. D. (1995). Pharmacology and neurochemistry of nefazodone, a novel antidepressant drug. *J. Clin. Psychiatry* **56,** 3–11.

Wallace, K. B., and Starkov, A. (2000). Mitochondrial targets of drug toxicity. *Annu. Rev. Pharmacol. Toxicol*. **40,** 353–388.

Westwood, F. R., Bigley, A., Randall, K., Marsden, A. M., and Scott, R. C. (2005). Statin-induced muscle necrosis in the rat: Distribution, development, and fibre selectivity. *Toxicol. Pathol*. **33,** 246–257.

Wilkening, S., Stahl, F., and Bader, A. (2003). Comparison of primary human hepatocytes and hepatoma cell line Hepg2 with regard to their biotransformation properties. *Drug Metab. Dispos*. **31,** 1035–1042.

Will, Y., Hynes, J., Ogurtsov, V. I., and Papkovsky, D. B. (2006). Analysis of mitochondrial function using phosphorescent oxygen-sensitive probes. *Nat. Protoc*. **1,** 2563–2572.